

Strong-coupling electron-phonon superconductivity in noncentrosymmetric quasi-one-dimensional $\text{K}_2\text{Cr}_3\text{As}_3$

Alaska Subedi

*Max Planck Institute for the Structure and Dynamics of Matter,
Luruper Chaussee 149, 22761 Hamburg, Germany*

(Dated: June 1, 2021)

I study the lattice dynamics and electron-phonon coupling in non-centrosymmetric quasi-one-dimensional $\text{K}_2\text{Cr}_3\text{As}_3$ using density functional theory based first principles calculations. The phonon dispersions show stable phonons without any soft-mode behavior. They also exhibit features that point to a strong interaction of K atoms with the lattice. I find that the calculated Eliashberg spectral function shows a large enhancement around 50 cm^{-1} . The phonon modes that show large coupling involve in-plane motions of all three species of atoms. The \mathbf{q} dependent electron-phonon coupling decreases strongly away from the $q_z = 0$ plane. The total electron-phonon coupling is large with a value of $\lambda_{\text{ep}} = 3.0$, which readily explains the experimentally observed large mass enhancement.

PACS numbers: 74.25.Kc

I. INTRODUCTION

Almost all known superconductors are conventional electron-phonon superconductors, and the phenomenon of unconventional superconductivity, especially in one-dimensional (1D) materials, is relatively unexplored. Therefore, the recent report of superconductivity that is likely of an unconventional nature in non-centrosymmetric quasi-1D $\text{K}_2\text{Cr}_3\text{As}_3$ with a T_c of 6.1 K by Bao *et al.* is of significant importance¹.

$\text{K}_2\text{Cr}_3\text{As}_3$ is structurally similar to the MMo_3X_3 or $\text{M}_2\text{Mo}_6\text{X}_6$ (M = metals, X = chalcogens) family of compounds first discovered in 1980^{2,3}. In addition to $\text{K}_2\text{Cr}_3\text{As}_3$, superconductivity has also been observed in two other isostructural compounds $\text{Rb}_2\text{Cr}_3\text{As}_3$ and $\text{Cs}_2\text{Cr}_3\text{As}_3$ with T_c 's of 4.8 and 2.2 K, respectively⁴⁻⁶. The one-dimensional element in $\text{A}_2\text{Cr}_3\text{As}_3$ ($A = \text{K}, \text{Rb}, \text{Cs}$) compounds is a $[(\text{Cr}_3\text{As}_3)^{2-}]_\infty$ chain, which is arranged in a hexagonal lattice. This chain has the structure of a double-walled subnanotube. The inner wall is made of stacked Cr_6 octahedra that are face-sharing along the c axis and the outer wall is made of similarly stacked face-sharing As_6 octahedra. The individual chains are separated by metal cations that provide the compensating charge and stabilize the structure.

The superconductivity in $\text{K}_2\text{Cr}_3\text{As}_3$ exhibits various features that are suggestive of an unconventional nature. The superconducting state arises out of a normal state that has a large specific heat coefficient of $70\text{--}75 \text{ mJ K}^{-2} \text{ mol}^{-1}$, which indicates strong quasiparticle mass renormalization^{1,7}. The upper critical field exceeds the one-band BCS estimate of the Pauli limit by a factor of $3\text{--}4$ ^{1,7-9}. NMR experiments show that spin fluctuations grow as the temperature approaches T_c ¹⁰. Below T_c , the nuclear spin-lattice relaxation rate does not show Hebel-Slichter coherence peak that is characteristic of an isotropic s -wave superconductor, and the relaxation rate decreases with a power-law behavior suggesting the presence of zero-energy excitations in the superconducting

state. The presence of zero-energy excitations is also seen in the temperature dependence of the penetration depth, which decreases linearly at temperatures well below T_c ¹¹. A fit of the angular dependence of the superconducting gap to the superfluid density obtained from the penetration depth shows reasonable agreement with various p -, d - and f -wave models that exhibit nodes. The temperature dependence of the superfluid density obtained from transverse-field μSR measurements show equally good fit to both an isotropic s -wave model and a d -wave model with line nodes¹². In addition, zero-field μSR measurements show a presence of internal magnetic field in the superconducting state, although the magnetic field is more than 100 times smaller than that observed in Sr_2RuO_4 . Raman scattering study of phonons with frequency greater than 100 cm^{-1} also show very weak electron-phonon coupling that is too small to account for the observed superconductivity in this material¹³. In addition to these experimental observations, various first principles and Hubbard model based theoretical studies also find that a triplet superconducting state mediated by magnetic fluctuations to be likely present in $\text{K}_2\text{Cr}_3\text{As}_3$ ¹⁴⁻¹⁹.

The experimental results that have so far been gathered on $\text{K}_2\text{Cr}_3\text{As}_3$ rule out an isotropic s -wave superconducting state in the weak-coupling limit, but they do not necessarily imply an unconventional 1D superconductivity mediated by magnetic fluctuations. Indeed, as pointed out by Balakirev *et al.*, the superconductivity in $\text{K}_2\text{Cr}_3\text{As}_3$ is inconsistent with such an unconventional superconducting state⁸. They find that the anisotropy of the upper critical field $\gamma_H(T) = H_{c2}^\perp/H_{c2}^\parallel$ is modest with $\gamma_H(T_c) \approx 0.35$ at T_c and $\gamma_H(0) \approx 1.5$ at 0.7 K, which suggests a rather three-dimensional nature of superconductivity. Even though $\text{K}_2\text{Cr}_3\text{As}_3$ is structurally very one-dimensional, first principles calculations show that the electronic structure is decidedly three-dimensional with the presence of a large three-dimensional Fermi sheet in addition to two one-dimensional sheets^{14,15}. Further-

more, the upper critical field parallel to the chain H_{c2}^{\parallel} is limited by Pauli pair breaking and is indicative of a singlet superconductivity, whereas the upper critical field perpendicular to the chain H_{c2}^{\perp} shows no Pauli pair breaking effects and is limited by orbital pair breaking⁸. In a quasi-1D superconductivity, H_{c2}^{\perp} would have been limited by orbital and Pauli pair breaking effects yielding $H_{c2}^{\perp} < H_{c2}^{\parallel}$. More importantly, superconductivity in $K_2Cr_3As_3$ has been observed in samples with residual resistivity ratio ranging from 10 to 50^{1,7-9}, but the T_c is essentially insensitive to the non-magnetic impurities. This suggests that the pairing is of s -wave type since scattering with non-magnetic impurities tends to average out the superconducting gap function, which would be detrimental to unconventional superconductors as their gap function has different signs in different regions of the Brillouin zone.

Motivated by these observations, I have investigated the lattice dynamics and electron-phonon coupling in $K_2As_3Cr_3$ using first principles density functional perturbation theory calculations. The phonon dispersions show the structure is stable, and there is an absence of a soft phonon behavior. Instead, they exhibit features that point to a strong coupling of K atoms with the lattice. The Eliashberg electron-phonon spectral function is strongly enhanced around 50 cm^{-1} . These phonons correspond to vibrations of all three constituent species and the coupling cannot be attributed to an Einstein-like rattling vibration. The phonon modes that exhibit large coupling are characterized by in-plane motion of the atoms. The \mathbf{q} dependent electron-phonon coupling is highly anisotropic. In particular, the coupling strongly decreases as one moves away from the $q_z = 0$ plane. The calculated total electron-phonon coupling $\lambda_{ep} = 3.0$ is large and readily explains the experimentally observed large mass enhancement.

II. COMPUTATIONAL APPROACH

The phonon dispersions and electron-phonon couplings presented here were obtained using density functional perturbation theory within the generalized gradient approximation (GGA) as implemented in the Quantum ESPRESSO package²⁰. I used the ultrasoft pseudopotentials generated by dal Corso²¹ and cutoffs of 50 and 500 Ry for basis-set and charge-density expansions, respectively. A $4 \times 4 \times 8$ grid was used for the Brillouin zone integration in the self-consistent calculations. The dynamical matrices were calculated on a $4 \times 4 \times 8$ grid and phonon dispersions and density of states are then obtained from Fourier interpolation. A denser $8 \times 8 \times 16$ grid and a smearing of 0.008 Ry was used in the calculation of the electron-phonon coupling. The electronic structure and structure relaxation calculations were also performed using the generalized full-potential method as implemented in the WIEN2k package²² as a check.

I used the experimental lattice parameters $a = 9.9832$

TABLE I: Relaxed internal parameters of $K_2Cr_3As_3$ using non-spin-polarized pseudopotential and full-potential calculations. The atomic coordinates in the $P\bar{6}m2$ space group are: As1 ($x, -x, 0$), As2 ($x, -x, 0.5$), Cr1 ($x, -x, 0.5$), Cr2 ($x, -x, 0$), K1 ($x, -x, 0.5$), K2 ($1/3, 2/3, 0$).

| | Wyckoff | x | x |
|-----|----------|-----------------|----------------|
| | position | pseudopotential | full-potential |
| As1 | 3j | 0.8345 | 0.8344 |
| As2 | 3k | 0.1667 | 0.1668 |
| Cr1 | 3k | 0.9175 | 0.9167 |
| Cr2 | 3j | 0.0859 | 0.0864 |
| K1 | 3k | 0.5380 | 0.5381 |

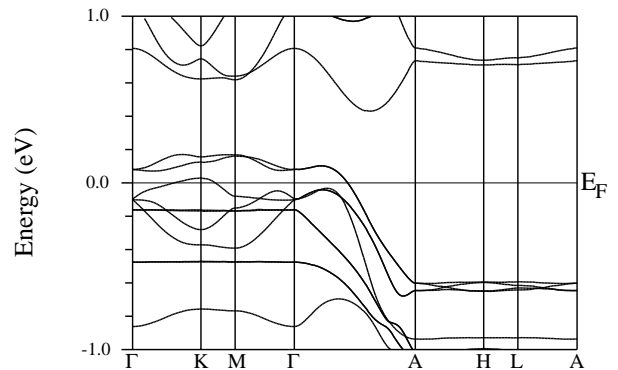


FIG. 1: Calculated GGA band structure of non-spin-polarized $K_2Cr_3As_3$ in the relaxed structure.

and $c = 4.2304$ Å but relaxed the internal atomic position parameters of the $P\bar{6}m2$ space group. The results of the geometry optimization calculations performed using both the pseudopotential and full-potential methods are summarized in Table I. These are in good agreement with each other and to the experimental values^{1,4}. Structural optimization leaves the As-As distances basically unchanged but reduces the Cr-Cr distances by 0.1 Å relative to the experimental values, in accord with a previous theoretical study¹⁵.

III. RESULTS AND DISCUSSION

The band structure and Fermi surface of $K_2As_3Cr_3$ calculated using the relaxed internal parameters are shown in Figs. 1 and 2, respectively. These differ in details from the ones presented in Refs. 14 and 15 that used experimental atomic positions. The one-dimensional nature of the material is evident from the relatively small dispersion along the in-plane Γ -K-M- Γ and A-H-L-A paths. However, some bands do show moderate dispersion along these paths, which indicates that the bonding between $[(Cr_3As_3)^{2-}]_{\infty}$ chains is substantial. The bands disperse strongly in the k_z direction (the Γ -A path), and

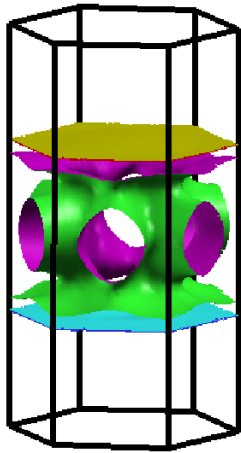


FIG. 2: (Color online) Calculated GGA Fermi surface of non-spin-polarized $\text{K}_2\text{Cr}_3\text{As}_3$ in the relaxed structure.

these reflect the short inter-atomic distances and strong bonding in the out-of-plane direction. I find substantial As p character above the Fermi level and the presence of large amount Cr d character in the lower part of the valence band manifold, which suggests that there is a strong covalency between Cr and As atoms. Even though the valence bands disperse relatively little in the in-plane directions, the valence band manifold extends from -4.8 to 0.2 eV and has a band width of 5.0 eV. This again reflects the strong covalency between Cr and As atoms. I obtain $N(E_F) = 6.94 \text{ eV}^{-1}$ per formula unit both spin basis for a value of the electronic density of states at the Fermi level. This corresponds to a calculated Sommerfeld coefficient of $\gamma = 16.36 \text{ mJ/mol K}^2$. The experimental γ obtained from specific heat capacity measurements is $\sim 70 \text{ mJ/mol K}^{21,7}$, and this corresponds to an enhancement by a factor of 4.3 relative to the calculated value.

There are three bands that cross the Fermi level, and these give rise to three Fermi sheets. The two upper-lying bands cross the Fermi level only along the k_z direction and give rise to a pair of 1D sheets. In my calculations these are degenerate, but they are non-degenerate in the calculations that use experimental atomic positions^{14,15}. The lower-lying band crosses the Fermi level around the K point, and this gives rise to a large three-dimensional sheet. Therefore, even though the structure of $\text{K}_2\text{Cr}_3\text{As}_3$ is quasi-1D, the material is very three-dimensional from the electronic structure point of view.

The phonon dispersions and density of states (pDOS) of $\text{K}_2\text{Cr}_3\text{As}_3$ are shown in Figs. 3 and 4, respectively. These again reflect the quasi-1D nature of the material as the in-plane dispersion of the optical branches is comparatively smaller than the out-of-plane dispersion. The strong bonding along the c axis is also seen in the large dispersion of the out-of-plane polarized acoustic mode along the q_z direction. This branch reaches more than

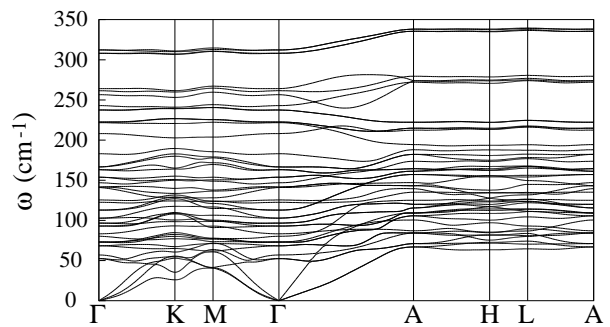


FIG. 3: Calculated GGA phonon dispersions of non-spin-polarized $\text{K}_2\text{Cr}_3\text{As}_3$.

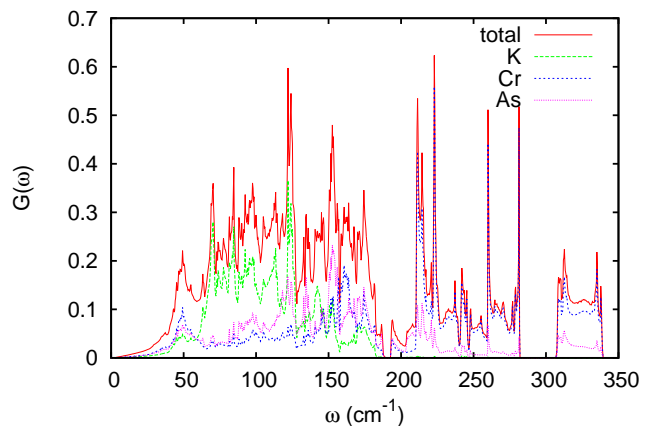


FIG. 4: (Color online) Calculated GGA phonon density of states of non-spin-polarized $\text{K}_2\text{Cr}_3\text{As}_3$.

100 cm^{-1} . Although the acoustic branches have smaller dispersion along the in-plane direction, these do not exhibit soft-mode behavior. This indicates weaker bonding between the $[(\text{Cr}_3\text{As}_3)^{2-}]_{\infty}$ chains, but it also implies that the structure is stable and not in a very close vicinity of a structural phase transition.

The pDOS exhibits many narrow peaks that are caused by narrow band widths of the phonon branches. The partial pDOS shows that the K atoms contribute to phonon modes up to 200 cm^{-1} . Therefore, the K atoms do not behave like a rattler that is weakly coupled to the lattice. The interaction with K ions is also seen in the stronger dispersion around the K point for branches below 200 cm^{-1} . The Cr and As atoms contribute to vibrations all across the phonon dispersion range. In particular, both Cr and As atoms contribute to the high-frequency phonon modes that again indicates strong covalency between these two.

The strength of the interaction between electrons and phonons is described in terms of the Eliashberg spectral

function:

$$\alpha^2 F(\omega) = \frac{1}{N(E_F)} \sum_{\mathbf{k}, \mathbf{q}, \nu, n, m} \delta(\epsilon_{\mathbf{k}}^n) \delta(\epsilon_{\mathbf{k}+\mathbf{q}}^m) |g_{\mathbf{k}, \mathbf{k}+\mathbf{q}}^{\nu, n, m}|^2 \delta(\omega - \omega_{\nu \mathbf{q}}), \quad (1)$$

where $N(E_F)$ is the electronic density of states at the Fermi level, $\epsilon_{\mathbf{k}}^n$ is the electronic energy at wavevector \mathbf{k} and band index n , $\omega_{\nu \mathbf{q}}$ is the energy of a phonon with wavevector \mathbf{q} and branch index ν , and $g_{\mathbf{k}, \mathbf{k}+\mathbf{q}}^{\nu, n, m}$ is the matrix element for an electron in the state $|n\mathbf{k}\rangle$ scattering to $|m\mathbf{k} + \mathbf{q}\rangle$ through a phonon $\omega_{\nu \mathbf{q}}$.

The calculated Eliashberg function is shown in Fig. 5. It shows that phonon at all frequencies contribute to the coupling, although the phonon modes around 50 cm^{-1} make an especially large contribution. The pDOS also shows a peak at this frequency. Similar low-energy peaks has also been observed in $M_2\text{Mo}_6X_6$ compounds, and they have been attributed to the Einstein-like vibrations of M atoms^{23,24}. However, we can see from Fig. 4 that the motion of all three types of atoms contribute to this low-energy peak in $\text{K}_2\text{Cr}_3\text{As}_3$. Therefore, even if these phonons have relatively small dispersion, the coupling cannot be ascribed to an Einstein-type rattling vibration of K atoms. I also investigated the polarization of the phonons that show large coupling to the electrons and find that these show strong in-plane character.

The \mathbf{q} dependent total electron-phonon coupling $\lambda_{\mathbf{q}}$ ($= \int_0^\infty d\omega \alpha^2 F(\omega, \mathbf{q})/\omega$) is plotted for the $q_z = 0$ and $\frac{\pi}{c}$ planes of the Brillouin zone in Fig. 6. I find that the variance of the coupling is large within a q_z plane. Furthermore, the coupling strongly decreases as one moves away from the Brillouin zone center along the q_z direction. This shows that the coupling is highly anisotropic, and it should also result in an anisotropic superconducting gap function. To find out which Fermi sheets contribute more to the total electron-phonon coupling, I calculated the partial electron-phonon couplings at several \mathbf{q} points by summing over the 1D and 3D Fermi sheets separately in Eq. 1. I find that the 3D sheet makes a dominant contribution to the coupling. Therefore, controlling the size of the 3D sheet by chemical doping, pressure or strain might be an effective way of enhancing or suppressing superconductivity. It will be interesting to see if magnetism or charge density wave order appears due to nesting between 1D sheets when the 3D sheet is suppressed.

I obtain a large value of $\lambda_{\text{ep}} = 3.0$ for the total electron-phonon coupling constant $\lambda_{\text{ep}} = \sum_{\mathbf{q}, \nu} \lambda_{\mathbf{q}, \nu} = 2 \int_0^\infty d\omega \alpha^2 F(\omega)/\omega$. The logarithmically averaged phonon frequency is $\omega_{\text{ln}} = 71 \text{ cm}^{-1}$. These can be used to estimate the T_c by using the simplified Allen-Dynes formula, even though the use of this formula is invalid in the present case of strong electron-phonon coupling that is highly anisotropic²⁵. The simplified Allen-Dynes formula has the form

$$T_c = \frac{\omega_{\text{ln}}}{1.2} \exp \left\{ -\frac{1.04(1 + \lambda_{\text{ep}})}{\lambda_{\text{ep}} - \mu^*(1 + 0.62\lambda_{\text{ep}})} \right\}.$$

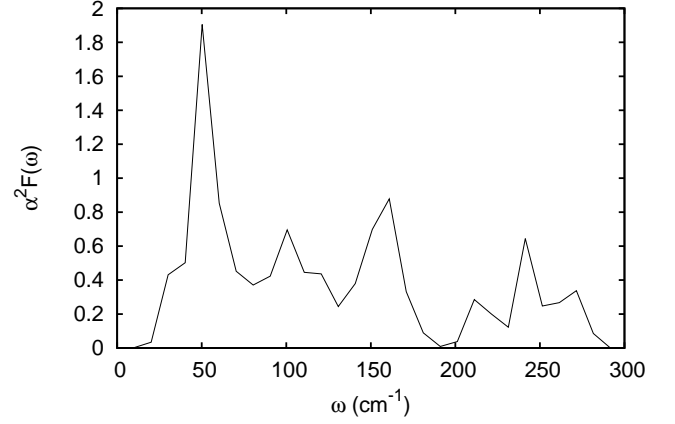


FIG. 5: Calculated Eliashberg spectral function of $\text{K}_2\text{Cr}_3\text{As}_3$.

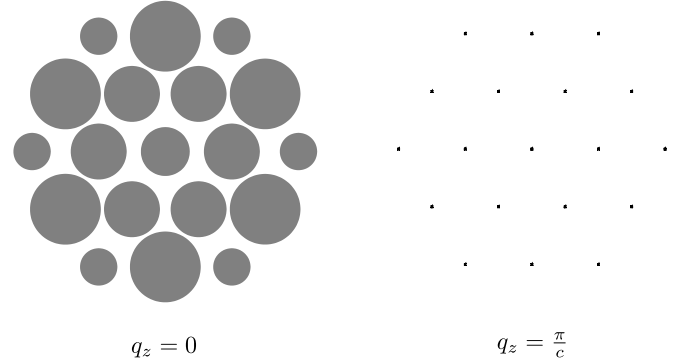


FIG. 6: Calculated \mathbf{q} dependent electron-phonon coupling $\lambda_{\mathbf{q}}$ shown for $q_z = 0$ and $q_z = \frac{\pi}{c}$ planes. The radius of the circle is proportional to the magnitude of $\lambda_{\mathbf{q}}$.

Using a value of $\mu^* = 0.12$ for the Coulomb pseudopotential parameter, I obtain $T_c = 17.8 \text{ K}$, which strongly overestimates the experimental T_c of 6 K. A full solution of the Migdal-Eliashberg equations, which is beyond the scope of this paper, will be required to obtain a more accurate T_c based on the calculated spectral function. Furthermore, there might be additional reasons for the overestimation of T_c . In the phonon calculations, I have neglected the phonon anharmonicities. This can raise the phonon frequencies, which will lower the total electron-phonon coupling. Another reason for the overestimation might be because I have neglected the effects of magnetic fluctuations. First principles calculations show the presence of various magnetic interactions with in this material^{14,15}, and this will also suppress T_c .

The calculated total electron-phonon coupling $\lambda_{\text{ep}} = 3.0$ readily explains the experimentally observed large electron mass enhancement from specific heat measurements. The electron-phonon coupling enhances the mass by a factor of $1 + \lambda_{\text{ep}} = 4.0$, which is very close to the experimentally observed mass enhancement factor of 4.3. Therefore, the large mass enhancement in this

material does not come from strong electronic correlations (in the sense of electron-electron interactions) or spin fluctuations. This is consistent with the experimentally estimated Wilson ratio of $R_W \approx 1^7$ that suggests a weak magnetic enhancement. The strong coupling nature of superconductivity in $\text{K}_2\text{Cr}_3\text{As}_3$ is also evident in the large jump of the dimensionless specific heat $\Delta C/\gamma T_c = 2.4^{1,7}$ at T_c . The strong electron-phonon coupling superconductivity proposed here can further be confirmed from tunneling experiments that should show a large value for the ratio $2\Delta(0)/T_c$, where $\Delta(0)$ is the superconducting gap.

Although the calculations presented here imply that the superconductivity in $\text{K}_2\text{Cr}_3\text{As}_3$ is caused by electron-phonon interactions, this does not necessarily mean that the superconductivity is dull or of the conventional BCS type. The crystal structure of this material lacks inversion symmetry, and parity is not a good quantum number in such a case. The pairing will likely have a dominant s character mixed with some p character. This can explain the presence of weak internal magnetic field below T_c in μSR measurements¹². In addition, the electron-phonon coupling is highly anisotropic, which can lead to accidental gaps in the superconducting state. This would be consistent with the signatures of nodes in the gap function in the NMR¹⁰ and penetration depth¹¹ measurements as well as the absence of Hebel-Slichter peak in the NMR measurements.

The presence of such a large electron-phonon coupling in this material provides an opportunity to study the properties of a superconducting state in the strong coupling limit. In particular, this may help explain why the measured upper critical fields H_{c2}^\perp and H_{c2}^\parallel greatly exceeds the Pauli limit estimated for a weakly-coupled isotropic BCS superconductor. It would be interesting to see if the fact that the coupling strongly decreases away from the $q_z = 0$ plane can explain why $H_{c2}^\parallel < H_{c2}^\perp$ in this material. These issues require more theoretical studies based on the full solution of Migdal-Eliashberg equations to be fully clarified.

As mentioned above, superconductivity is also observed in other inorganic quasi-1D compounds including $\text{Ti}_2\text{Mo}_6\text{Se}_6$ and $\text{Li}_{0.9}\text{Mo}_6\text{O}_{17}$, and the nature of their pairing interaction has not been fully elucidated. The results of phonon dispersions and electron-phonon coupling for $\text{K}_2\text{Cr}_3\text{As}_3$ presented here provides a reference

case for other quasi-1D superconductors. In particular, the present study shows that a behavior that deviates from what is expected from a weakly-coupled isotropic s -wave BCS superconductor does not necessarily imply that the superconductivity is mediated by magnetic interactions.

IV. SUMMARY AND CONCLUSIONS

In summary, I have investigated the lattice dynamics and electron-phonon coupling in $\text{K}_2\text{Cr}_3\text{As}_3$ using first principles calculations. The phonon dispersions do not show closeness to a lattice instability and exhibits features pointing to a strong coupling of K atoms with the lattice. The Eliashberg spectral function is strongly enhanced around 50 cm^{-1} , but there is coupling to high frequency phonons as well. The peak in the spectral function corresponds to the vibrations of all three constituent atomic species of the material. Although the electrons do not predominantly couple to vibrations of any specific atoms, vibrations that involve in-plane motion of atoms show strong electron-phonon coupling. The electron-phonon coupling shows strong \mathbf{q} dependence, especially along the out-of-plane direction. The calculated total-electron phonon coupling $\lambda_{\text{ep}} = 3.0$ is large and is consistent with the experimentally observed large mass enhancement and jump in the specific heat at T_c ^{1,7}. These calculations motivate tunneling experiments that can further confirm the strong coupling nature of superconductivity in this material by displaying an enhanced value of the ratio $2\Delta(0)/T_c$. The electron-phonon spectral function can also be extracted from such experiments, and they can be compared with the results presented here to validate the strong electron-phonon coupling scenario proposed here.

V. ACKNOWLEDGMENTS

I am grateful to David J. Singh for helpful discussions and suggestions. This work was supported by the Swiss National Supercomputing Centre (CSCS) under project ID s575 and by a grant from the European Research Council (ERC-319286 QMAC).

-
- ¹ J.-K. Bao, J.-Y. Liu, C.-W. Ma, Z.-H. Meng, Z.-T. Tang, Y.-L. Sun, H.-F. Zhai, H. Jiang, H. Bai, C.-M. Feng, Z.-A. Xu, and G.-H. Cao, Phys. Rev. X **5**, 011013 (2015).
 - ² M. Potel, R. Chevrel, M. Sergent, J. Armici, M. Decroux, and Ø. Fischer, J. Solid State Chem. **35**, 286 (1980).
 - ³ W. Hönle, H. von Schnering, A. Lipka, and K. Yvon, J. Less-Common Met. **71**, 135 (1980).
 - ⁴ Z.-T. Tang, J.-K. Bao, Y. Liu, Y.-L. Sun, A. Ablimit, H.-F. Zhai, H. Jiang, C.-M. Feng, Z.-A. Xu, G.-H. Cao, Phys.

- Rev. B **91**, 020506(R) (2015).
- ⁵ Z.-T. Tang, J.-K. Bao, Z. Wang, H. Bai, H. Jiang, Y. Liu, H.-F. Zhai, C.-M. Feng, Z.-A. Xu, and G.-H. Cao, Sci. China Mater. **58**, 16 (2015).
- ⁶ Z.-T. Tang, J.-K. Bao, Y. Liu, H. Bai, H. Jiang, H.-F. Zhai, C.-M. Feng, Z.-A. Xu, G.-H. Cao, Sci. China Mater. (2015)
- ⁷ T. Kong, S. L. Bud'ko, and P. C. Canfield, Phys. Rev. B **91**, 020507(R) (2015).

- ⁸ F. F. Balakirev, T. Kong, M. Jaime, R. D. McDonald, C. H. Mielke, A. Gurevich, P. C. Canfield and S. L. Bud'ko, *Phys. Rev. B* **91**, 220505(R) (2015).
- ⁹ X. F. Wang, C. Roncaioli, C. Eckberg, H. Kim, J. Yong, Y. Nakajima, S. R. Saha, P. Y. Zavalij, and J. Paglione, *Phys. Rev. B* **92**, 020508(R) (2015).
- ¹⁰ H. Z. Zhi, T. Imai, F. L. Ning, J.-K. Bao, and G.-H. Cao, *Phys. Rev. Lett.* **114**, 147004 (2015).
- ¹¹ G. M. Pang, M. Smidman, W. B. Jiang, J. K. Bao, Z. F. Weng, Y.F. Wang, L. Jiao, J. L. Zhang, G. H. Cao, and H. Q. Yuan, *Phys. Rev. B* **91**, 220502(R) (2015).
- ¹² D. T. Adroja, A. Bhattacharya, M. Telling, Yu. Feng, M. Smidman, B. Pan, J. Zhao, A. D. Hillier, F. L. Pratt, and A. M. Strydom, *cond-mat*, arXiv:1505.05743 (2015).
- ¹³ W.-L. Zhang, H. Li, D. Xia, H. W. Liu, Y.-G. Shi, J. L. Luo, J. Hu, P. Richard, H. Ding, *cond-mat*, arXiv:1506.01121 (2015).
- ¹⁴ H. Jiang, G. Cao, and C. Cao, *cond-mat*, arXiv:1412.1309 (2014).
- ¹⁵ X.-X. Wu, C.-C. Le, J. Yuan, H. Fan, J.-P. Hu, *Chin. Phys. Lett.* **32** 057410 (2015).
- ¹⁶ Y. Zhou, C. Cao, and F.-C. Zhang, *cond-mat*, arXiv:1502.03928 (2015).
- ¹⁷ X.-X. Wu, C.-C. Le, H. Fan, J.-P. Hu, *cond-mat*, arXiv:1503.06707 (2015).
- ¹⁸ H. Zhong, X.-Y. Feng, H. Chen, J. Dai, *cond-mat*, arXiv:1503.08965 (2015).
- ¹⁹ X.-X. Wu, F. Yang, S.-S. Qin, H. Fan, J.-P. Hu, *cond-mat*, arXiv:1507.07451 (2015).
- ²⁰ P. Giannozzi, S. Baroni, N. Bonini, M. Calandra, R. Car, C. Cavazzoni, D. Ceresoli, G. L. Chiarotti, M. Cococcioni, I. Dabo *et al.*, *J. Phys.: Condens. Matter* **21**, 395502 (2009).
- ²¹ A. dal Corso, *Comput. Mater. Sci.* **95**, 337 (2014).
- ²² P. Blaha, K. Schwarz, G. Madsen, D. Kvasnicka, and J. Luitz, "WIEN2k, An Augmented Plane Wave + Local Orbitals Program for Calculating Crystal Properties" (K. Schwarz, Tech. Univ. Wien, Austria) (2001).
- ²³ R. Brusetti, A. J. Dianoux, P. Gougeon, M. Potel, E. Bonjour, and R. Calemczuk, *Phys. Rev. B* **41**, 6315 (1990).
- ²⁴ A. P. Petrović, R. Lortz, G. Santi, M. Decroux, H. Monnard, Ø. Fischer, L. Boeri, O. K. Andersen, J. Kortus, D. Salloum, P. Gougeon, and M. Potel, *Phys. Rev. B* **82**, 235128 (2010).
- ²⁵ J. P. Carbotte, *Rev. Mod. Phys.* **62**, 1027 (1990).